J Mater Sci (2011) 46:145–154
DOI 10.1007/s10853-010-4881-x

Cyclic hardening and fatigue behavior of stainless steel 304L

Julie Colin · Ali Fatemi · Said Taheri

Received: 11 June 2010 / Accepted: 30 August 2010 / Published online: 14 September 2010

Abstract This article discusses cyclic hardening and fatigue behaviors of stainless steel 304L, the behavior of which is greatly influenced by prior loading. Effects of loading sequence, mean strain and mean stress, and pre-straining (PS) were investigated using constant amplitude as well as step and random loading tests. Contrary to common expectations, fatigue lives in strain-controlled mean strain tests were significantly affected by the mean strain, in spite of mean stress relaxation. PS induced considerable hardening and led to different results on fatigue life, depending on the test control mode. Secondary hardening was observed in some tests, characterized by a continuous increase in the stress response. Possible mechanisms for this behavior are also discussed. To correlate fatigue life data of a material such as stainless steel with strong deformation history effect, it is shown that a damage parameter with both stress and strain is required. The Fatemi–Socie (FS) parameter as such a parameter is shown to correlate the data under different control modes and loading conditions.

List of symbols

b	Fatigue strength exponent
c	Fatigue ductility exponent
D	Damage ratio
E, E'	Monotonic, cyclic modulus of elasticity
K, K'	Monotonic, cyclic strength coefficient
n, n'	Monotonic, cyclic strain hardening exponent
n_i	Number of cycles applied at a given level
N	Number of cycles
N_f, $2N_f$	Number of cycles, reversals to failure
R_ε, R_σ	Strain, stress ratio
% RA	Percent reduction in area
S_u	Ultimate tensile strength
S_y, S_y'	Monotonic, cyclic yield strength
ε_f, ε_f'	True fracture ductility, fatigue ductility coefficient
ε_a, ε_m	Strain amplitude, mean strain
ε_{max}, ε_{min}	Maximum, minimum strain
ΣD	Damage sum (using LDR)
σ_f, σ_f'	True fracture strength, fatigue strength coefficient
σ_a, σ_m	Stress amplitude, mean stress
σ_{max}, σ_{min}	Maximum, minimum stress
$\Delta\gamma_{max}$	Maximum shear strain range
ν_e, ν_p	Elastic, plastic Poisson's ratio

Abbreviations

CA	Constant amplitude
fcc	Face-centered cubic
FR	Fully reversed
FS	Fatemi–Socie
HCF	High cycle fatigue
H–L	High–low
LC	Load-controlled
LDR	Linear damage rule
L–H	Low–high
PS	Pre-straining
RL	Random loading
SFE	Stacking fault energy

J. Colin · A. Fatemi (✉)
Mechanical, Industrial and Manufacturing Engineering Department, The University of Toledo, 2801 West Bancroft Street, Toledo, OH 43606, USA
e-mail: afatemi@eng.utoledo.edu

S. Taheri
LaMSID, Common Research Laboratory CNRS-EDF, 2832 Electricité de France, Department AMA, 1 Avenue du Général de Gaulle, 92141 Clamart Cedex, France

SWT Smith–Watson–Topper
εC Strain-controlled
V Virgin material

Introduction

Deformation or load history effect of a material on subsequent cyclic loading depends on the degree of cyclic hardening, which in turn depends on how easy the dislocations can cross slip. For face-centered cubic (fcc) metals, the ease of cross slip depends on the stacking fault energy (SFE) of the material. In metals with low SFE, such as austenitic stainless steels, cross slip is difficult, while planar slip occurs readily. The deformation behavior is, therefore, greatly dependent on the loading history.

Stainless steel 304 is used in many applications where corrosion resistance and high toughness are important. As an austenitic steel, the deformation behavior greatly depends on the loading history. Among others, Lieurade and co-workers have reported strong deformation history effects on fatigue behavior of austenitic stainless steels 304 and 316 [1].

Stainless steel 304L also presents the characteristic of undergoing stress- or strain-induced phase transformation. Under cyclic loading, this is exhibited by significant hardening related to martensitic transformation, the extent of which has been associated with the amplitude of plastic deformation, as well as with the amount of cumulative plastic strain [2]. Such transformation can, therefore, occur in both low cycle as well as high cycle fatigue (HCF).

An important microstructural modification in austenitic stainless steels has been identified with a phenomenon known as secondary hardening in HCF. This is characterized by a significant cyclic hardening with continued cycling, as well as extension of fatigue life. It has been suggested that this might be associated with the formation of a specific microstructure referred to as a corduroy structure [3].

Micro- and/or macro-crack growth, which can constitute a significant portion of fatigue life in stainless steel, can also be affected by microstructural alterations. Khan and Ahmed [4] studied crack growth of single-edge notched stainless steel specimens under variable amplitude loading and concluded that two mechanisms may occur. The first mechanism is beneficial, where martensitic transformation which induces an increase in the specific volume creates compressive residual stresses at the crack tip, hence limiting crack growth. The other phenomenon is a reduced ductility due to the hardening from martensitic transformation and is detrimental since it allows faster crack growth. The relative contribution of the two phenomena depends on the applied strain amplitude [4].

This article discusses deformation history effects on stainless steel 304L due to pre-hardening, as well as mean stress and mean strain effects, and load sequence effects on fatigue life. Pre-hardening and loading sequence can have a substantial influence on deformation and fatigue behaviors of materials with strong deformation history effect, where the amplitude of preloading and overload cycles determine to what extent the material behavior will be affected [5]. Mean stress can also have significant effects on both deformation and fatigue behaviors. A compressive mean stress is generally beneficial to fatigue life, whereas a tensile mean stress is detrimental to fatigue life [6].

The stainless steel 304L used in this study had low carbon and a chemical composition of 0.023% C, 1.13% Mn, 0.49% Si, 0.004% S, 0.024% P, 10.1% Ni, 18.5% Cr, 0.09% Mo, 0.1% Cu, and 0.028% N_2. Tensile properties are listed in Table 1. In addition to fully reversed constant amplitude strain-controlled fatigue tests, some fully reversed tests were also conducted in load control in order to investigate the influence of the test control mode. The load levels used in load-controlled tests were obtained from the midlife stress values in strain-controlled tests.

The experimental program also included high–low (H–L) step tests and random loading (RL) tests. To evaluate fatigue life under variable amplitude or RL, the Palmgren–Miner linear damage rule (LDR) was used due to its universality of use and ease of application [7]. This rule considers damage, quantified as damage fraction or cycle ratio, to accumulate in a linear fashion.

Table 1 Mechanical and strain-controlled fatigue properties of stainless steel 304L

Monotonic properties	
Modulus of elasticity, E (GPa)	193
Yield strength (0.2% offset), S_y (MPa)	202
Ultimate tensile strength, S_u (MPa)	608
Percent reduction in area, %RA	83
Strength coefficient, K (MPa)	804
Strain hardening exponent, n	0.255
True fracture strength, σ_f (MPa)	1763
True fracture ductility, ε_f (%)	178
Cyclic properties	
Cyclic modulus of elasticity, E' (GPa)	193
Fatigue strength coefficient, bilinear fit, $\sigma'_{f_1}/\sigma'_{f_2}$ (MPa)	2,558/819
Fatigue strength exponent, bilinear fit, b_1/b_2	−0.239/−0.104
Fatigue ductility coefficient, $\varepsilon'_{f_1}/\varepsilon'_{f_2}$	0.522/0.0242
Fatigue ductility exponent, c_1/c_2	−0.557/−0.203
Cyclic strength coefficient, bilinear fit, K' (MPa)	2,224
Cyclic strain hardening exponent, bilinear fit, n'	0.341
Cyclic yield strength, S_y' (MPa)	238

Identical cylindrical smooth solid specimens were used in all experiments. Specimens were machined from 3-cm thick plates in the rolling direction. Triangular waveform was used and cyclic frequencies ranged between 0.35 and 7 Hz, depending on the total strain amplitude, in order to have similar strain rates. Details of the specimen geometry, test equipment, and experimental procedures used are reported in [8, 9]. It should be mentioned that the results for the stainless steel 304L reported in this article are for the THYSSEN grade, while the results reported in [8, 9] are for the Creusot Loire Industrie (CLI) grade of stainless steel 304L.

Cyclic deformation behavior

An incremental step test was conducted, where a single specimen was subjected to increasing and then decreasing strain amplitudes. Each strain amplitude level was maintained for a number of cycles large enough to obtain a fairly constant response (i.e., saturated response). As expected, the stress response, as shown in Fig. 1, is strongly affected by the prior higher strain amplitude cycles in the straining sequence. This is explained in terms of the low SFE of stainless steel, as discussed earlier, where cross slip is difficult, resulting in deformation behavior dependent on the prior loading.

Figure 2a shows superimposed midlife hysteresis loops at different strain amplitudes, where considerable plastic deformation is observed, even at low strain amplitude of 0.25%, which was the runout fatigue test level for the material. Superimposed stable cyclic (obtained from midlife data) and tensile stress–strain curves are shown in Fig. 2b, where strong cyclic hardening is observed. This hardening becomes more significant at higher strain amplitudes (about 100% hardening at 2% strain amplitude).

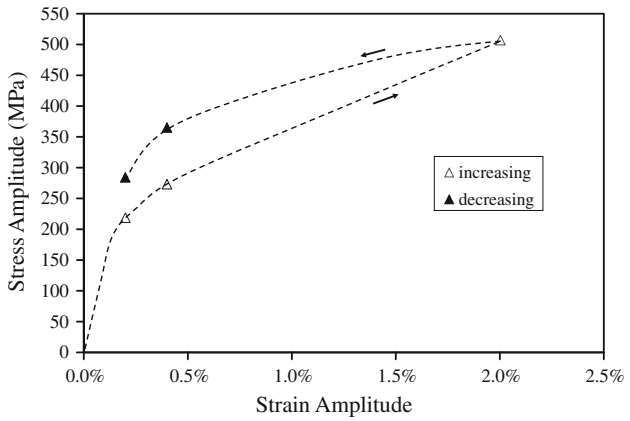

Fig. 1 Superimposed stress response in incremental step test in strain control

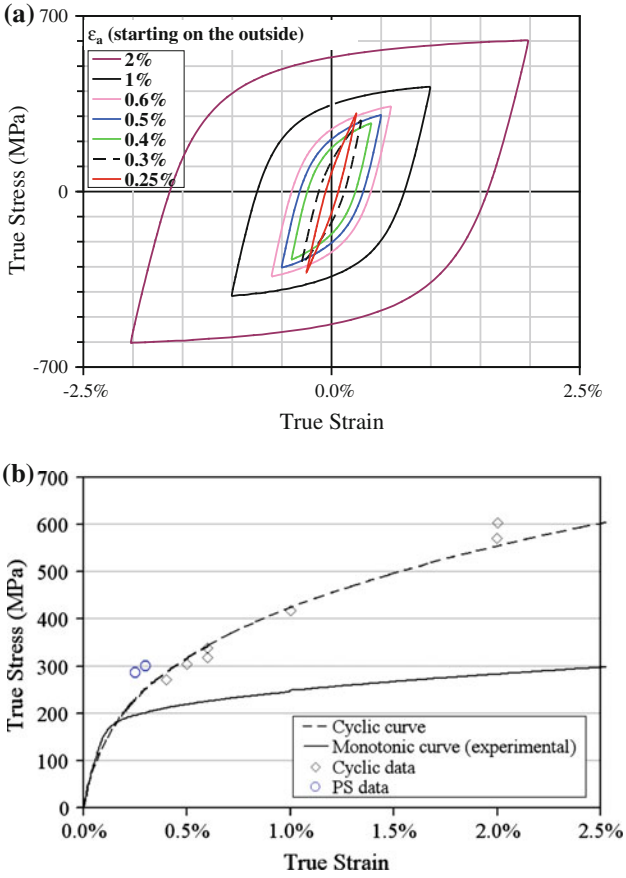

Fig. 2 Superimposed midlife hysteresis loops from constant amplitude fatigue tests (**a**) and superimposed monotonic and cyclic stress–strain curves and data

Constant amplitude fatigue behavior

All constant amplitude fatigue test results are shown in Table 2, where true stress and true strain values reported were obtained from midlife cycles. Figure 3 represents the strain–life curve obtained from fully-reversed constant amplitude strain-controlled (εC) fatigue tests. The few load-controlled (LC) test data are on the strain–life curve. Therefore, the test control mode (i.e., strain or load) has no effect on the behavior of the material under constant amplitude fully reversed loading. Fatigue properties obtained from the midlife data are listed in Table 1. Due to the bilinearity of the elastic and plastic curve data fits, two sets of values are listed for strain–life properties. The first set (with subscript 1) applies to fatigue lives <5,000 reversals to failure, while the second set (with subscript 2) applies to longer fatigue lives.

Mean strain effects

Mean strain tests in strain control were conducted with R_ε ratios of ∞, 0, and 0.75, all at strain amplitude of about

Table 2 Fatigue tests results including fully reversed constant amplitude, mean stress, and pre-strained tests

Control mode	R	ε_a (%)	ε_m (%)	σ_a (MPa)	σ_m (MPa)	$2N_f$
Strain	−1	2.00	−0.02	571	1.0	442
Strain	−1	2.00	−0.02	603	0.3	468
Strain	−1	1.00	0.00	417	1.3	1,950
Strain	−1	1.00	−0.01	417	0.4	2,308
Strain	−1	0.600	0.00	339	0.7	5,478
Strain	−1	0.600	0.00	317	0.8	5,140
Strain	−1	0.500	0.00	304	0.9	21,886
Strain	−1	0.400	0.00	271	0.9	43,414
Strain	−1	0.400	0.00	271	5.6	34,590
Strain	−1	0.300	0.00	287	−2.3	1,057,360
Strain	−1	0.300	0.00	261	−0.4	625,746
Strain	−1	0.250	0.00	316	−4.6	>4,043,156
Load	−1	0.455	0.09	300	1.5	26,250
Load	−1	0.431	0.21	301	1.3	37,252
Load	−1	0.407	0.11	274	1.2	46,882
Load	−1	0.410	0.10	275	0.9	40,400
Mean strain tests						
Strain	∞	0.301	−0.30	475	−14.8	>8,354,260
Strain	0	0.299	0.30	234	2.0	177,882
Strain	0	0.299	0.30	239	1.5	256,188
Strain	0.75	0.294	2.08	257	6.4	107,410
Strain	0.75	0.294	2.08	255	7.6	113,610
Pre-strained tests[a]						
Strain	−1	0.300	−0.06	301	0.3	157,792
Strain	−1	0.300	−0.06	299	0.4	139,132
Strain	−1	0.250	−0.04	285	14.7	289,914
Strain	−1	0.250	−0.04	286	−2.6	416,224
Load	−1	0.186	−0.04	276	0.4	>6,323,860

[a] Pre-straining was conducted at 2% strain amplitude for 10 cycles

0.3%. The ratio of ∞ indicates straining between −0.6% and 0, the ratio of 0 indicates straining between 0 and 0.6%, and the ratio of 0.75 indicates straining between 1.8 and 2.4%. Results from these tests are included in Table 2. Due to considerable amount of cyclic plasticity, the mean stress relaxed to very low values (<15 MPa) during the first few percent of the fatigue life in all mean strain tests.

Fatigue data from mean strain tests are also shown in Fig. 3. The R_ε ratios of 0 and 0.75 (i.e., tensile mean strain) resulted in factors of 4 and 8 shorter fatigue lives, compared to the fully reversed ($R_\varepsilon = -1$) straining, respectively. In contrast, the R_ε ratio of ∞ (i.e., compressive mean strain) resulted in more than an order of magnitude longer life than the fully reversed test, and the specimen did not fail after more than 4 million cycles. These results are in spite of the fact that the mean stress in all mean strain tests nearly fully relaxed. Therefore, the large differences

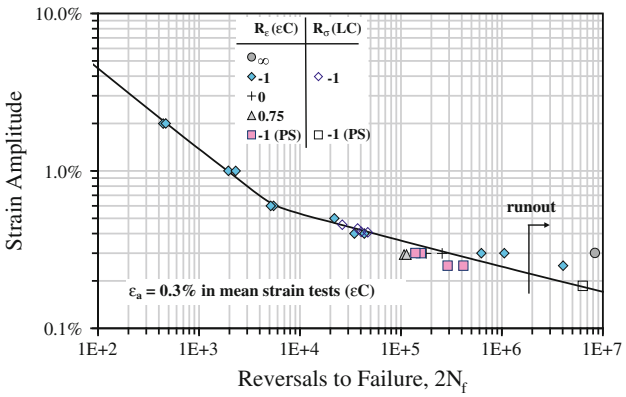

Fig. 3 Strain–life behavior including all constant amplitude tests data

in fatigue lives observed between the different mean strain tests are merely due to the differences in mean strain. This is contrary to the common expectation that mean strain has an effect on fatigue life only if it induces a non-relaxing mean stress [6]. Possible microstructure alterations, such as phase transformation and/or changes in dislocation structure, may explain this surprising behavior under mean strain (but no mean stress) conditions.

Pre-straining effects

The influence of pre-straining (PS) was investigated by PS specimens in strain control and then fatigue testing under either load control or strain control. These tests were conducted with 10 pre-strain cycles at 2% total strain amplitude. Results for pre-strained tests are also included in Table 2 and are from midlife constant amplitude cycles following PS.

Midlife stress amplitudes from fully reversed strain-controlled tests on pre-strained specimens presented in Fig. 2b indicate hardening from PS cycles at higher strain amplitude, as pre-strained test data are above the cyclic stress–strain curve. For the load-controlled test, the pre-strained specimen had a smaller strain amplitude (0.186%) than that of the virgin specimens at identical stress level (0.41%, see Table 2). The strain amplitude was found to be a more significant factor than the maximum strain with respect to the resulting hardening.

The effect of PS on fatigue life was dependent on the test control mode. PS led to significantly shorter life in strain-controlled tests (by a factor of more than 5), but significantly longer life in load-controlled test (by more than two orders of magnitude), as compared with the virgin material (i.e., without pre-cycling), see Fig. 3 and Table 1. Therefore, using a damage parameter that considers both stress and strain is a more appropriate approach, than using either strain or stress individually, for fatigue life prediction and correlating load- and strain-controlled fatigue data.

Fatigue life correlations

Two common fatigue damage parameters which include both stress and strain terms are the Smith–Watson–Topper (SWT) [10] and the Fatemi–Socie (FS) [11] parameters. Although the FS parameter is a multiaxial fatigue parameter, this parameter can also be used for uniaxial data correlations. The FS parameter is given by:

$$\frac{\Delta\gamma_{\max}}{2}\left(1+k\frac{\sigma_{n,\max}}{S_y}\right) = \left[(1+\nu_e)\frac{\sigma_f'}{E}(2N_f)^b+(1+\nu_p)\varepsilon_f'(2N_f)^c\right] \times\left[1+k\frac{\sigma_f'}{2S_y}(2N_f)^b\right], \quad (1)$$

where $\sigma_{n,\max} = \sigma_{n,a} + \sigma_{n,m}$, with $\sigma_{n,m}$ being the mean stress and being the $\sigma_{n,a}$ alternating stress. This parameter can, therefore, also take into account mean stress effects. In this equation, the first set of fatigue properties in Table 1 are used for lives shorter than 5,000 reversals to failure, and the second set of properties are used for longer lives, as previously discussed. The yield strength, S_y, is also listed in Table 1. A typical value of $k = 1$ was used, as applied to this material.

Figure 4 shows all the constant amplitude fatigue data superimposed on FS–life plot. Although good data correlations are obtained, data from tests exhibiting secondary hardening, particularly the runout test data, are not near the curve. This, however, is not due to a shortcoming of this or other similar damage parameters. Instead, this is due to the fact that such data are not included in data fits used to obtain the material fatigue properties listed in Table 1. These properties are subsequently used to construct the FS–life curve shown in Fig. 4. Data correlations obtained with the SWT parameter were similar to those shown in Fig. 5.

Secondary hardening

The material exhibited secondary hardening in several tests with strain amplitudes at or below 0.3%. In such cases, after a period of initial softening, a second period of hardening was observed that continued throughout the tests. Stress amplitude response of tests with secondary hardening is shown in Fig. 5, including fully reversed tests at 0.25 and 0.3% strain amplitudes as well as the mean strain test with $R_\varepsilon = \infty$. In addition to the considerable continued hardening, significant increases in fatigue lives were also observed in such tests.

Some researchers have postulated the importance of cumulative plastic strain in martensitic transformation. A cumulative plastic strain amplitude threshold can be defined that depends on different factors, including the composition of the austenitic stainless steel [2]. Nickel, chromium, and most particularly carbon are known to stabilize the austenite phase [12, 13]. In the present study, cumulative plastic strain amplitude ($N\ \Delta\varepsilon_p/2$) was computed for all tests and plotted versus number of cycles to failure as shown in Fig. 6. From this plot a threshold was identified (at 60), above which secondary hardening was most likely to occur. While this threshold value can be used to predict when secondary hardening may start, it does not predict if, or explain why, it does occur.

During martensitic transformation, two types of martensite can form, the α' phase (bcc) and the ε phase (hc) [13–15]. The α' phase is ferro-magnetic [15] and can be easily detected. In this investigation, qualitative magnetic measurements were made on different tested specimens using a commercial magnetometer. Strong magnetization was observed for specimens cycled at high strain amplitudes, and for specimens which exhibited secondary hardening.

In an attempt to further characterized secondary hardening, micro-hardness (Vickers hardness) was measured

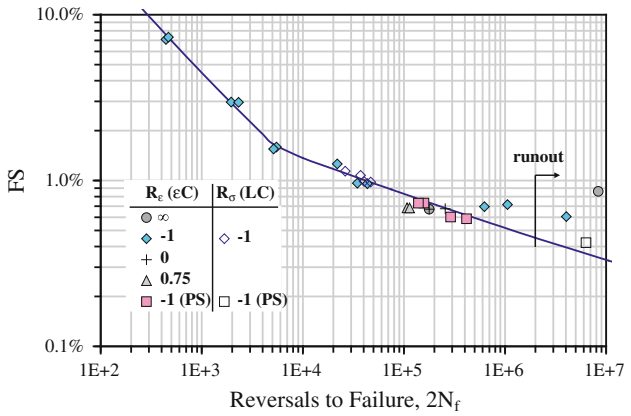

Fig. 4 FS parameter versus reversals to failure including all constant amplitude tests data

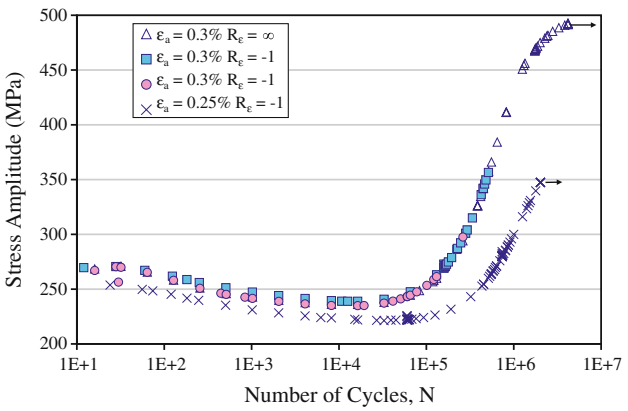

Fig. 5 Stress response for tests presenting secondary hardening

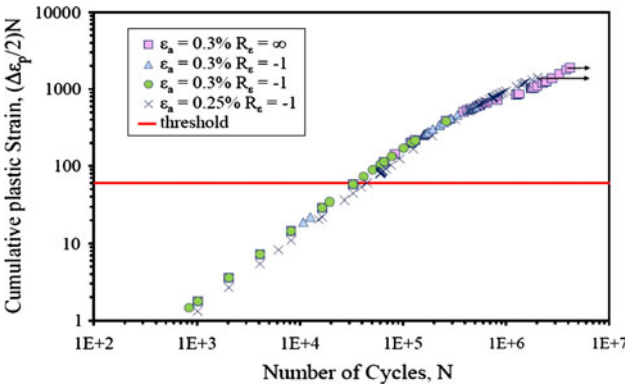

Fig. 6 Cumulative plastic strain in tests conducted at strain amplitude levels where secondary hardening was observed

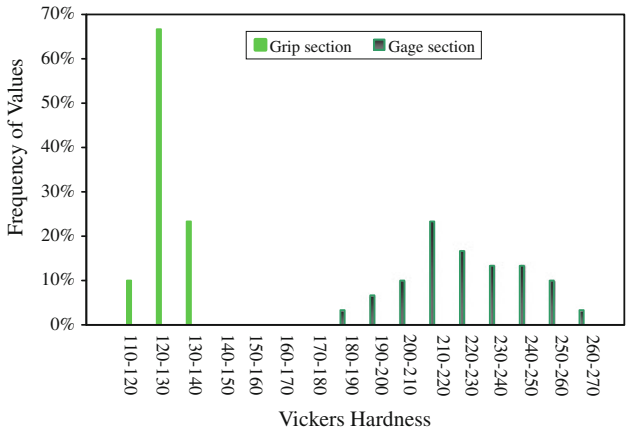

Fig. 7 Distributions of Vickers hardness measurements across the gage section and the grip section of a specimen tested at fully reversed 0.25% constant strain amplitude and exhibiting secondary hardening

across the grip section and across the gage section of a runout specimen exhibiting secondary hardening. This specimen was tested in strain control at 0.25% strain amplitude under constant amplitude fully reversed conditions. The distributions for micro-hardness measurements are shown in Fig. 7. The differences in mean hardness between gage section and grip section can be explained by the differences in stresses observed in the two parts of the specimen, arising from much larger diameter in the grip section, as compared to the gage section. The higher variation in hardness observed for the gage section, and characterized by a broader distribution of hardness values, can only be attributed to heterogeneity in the material. Since the grip section was more homogeneous, as indicated by a narrow distribution of hardness values for this section, heterogeneity of the gage section is most likely due to scattered martensitic transformation within this region, as this is a local phenomenon. The higher Vickers hardness values most probably correspond to regions where phase transformation occurred.

The effect of secondary hardening on the stiffness of SS304L was also studied by evaluating changes in elastic modulus, measured from experimental hysteresis loops. However, due to the absence of a clear trend in stiffness behavior, no conclusion could be made based on changes in stiffness.

As discussed earlier, martensitic transformation might not entirely explain secondary hardening and other microstructure alterations could also co-occur in the material [3]. PS can induce sufficient initial hardening to prevent or hinder additional alterations of the microstructure by cycling at lower strain amplitude. This occurred in strain control at strain amplitude of 0.25%, where PS prevented the occurrence of secondary hardening which was observed for the virgin material at this strain amplitude (see Table 2).

Variable amplitude fatigue behavior

High–low (H–L) sequence step tests

High–low step tests at different levels and with different damage ratios were conducted in either strain control or load control. In strain control, a gradual decrease of the higher strain amplitude to zero before starting to apply the lower strain amplitude cycles avoided a mean stress at the lower strain amplitude level [16].

Experimental test conditions and results for the step tests are gathered in Table 3, where tests are grouped by test

Table 3 Summary of high–low (H–L) step tests results

Control mode	$\varepsilon_{a_1}/\varepsilon_{a_2}$ (%)	$\varepsilon_{m_1}/\varepsilon_{m_2}$ (%)	n_1/n_2	$\sigma_{a_1}/\sigma_{a_2}$ (MPa)	$\sigma_{m_1}/\sigma_{m_2}$ (MPa)	D_1/D_2 (ε–N or S–N)	ΣD (ε–N or S–N)	ΣD (FS)
Strain	1.00/0.300	−0.01/0.00	107/57,306	389/265	0.5/0.5	0.10/0.14	0.24	0.70
Strain	1.00/0.300	−0.01/0.00	107/66,606	388/262	0.9/1.2	0.10/0.16	0.26	0.79
Strain	1.00/0.300	−0.01/0.00	530/34,597	415/290	0.8/2.0	0.50/0.08	0.58	1.00
Strain	1.00/0.300	0.00/0.00	530/31,332	416/289	0.4/1.1	0.50/0.07	0.57	0.96
Load	1.03/0.229	1.78/1.28	212/215,932	424/278	4.3/0.6	0.20/9.90	10.10	0.82
Load	1.08/0.228	2.59/2.05	212/227,745	428/280	4.7/0.6	0.20/10.44	10.64	0.87

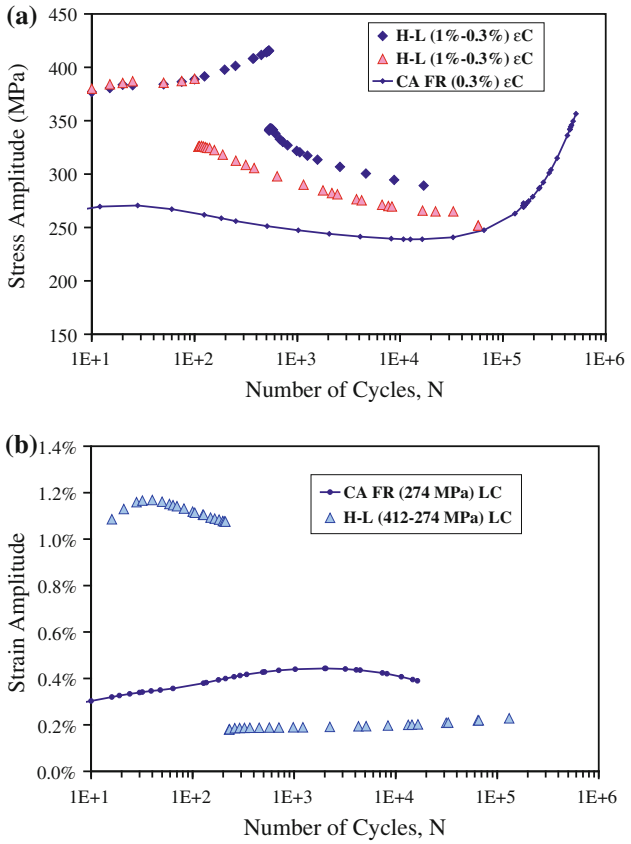

Fig. 8 Stress responses from strain-controlled high–low (H–L) step tests (**a**), and strain responses from load-controlled H–L step tests (**b**), as a function of number of cycles. Fully reversed (FR) constant amplitude (CA) response is also shown as reference for comparison with the second step

control mode. Stress or strain values listed represent the stabilized response, and damage ratios were calculated using the LDR, with different approaches (i.e., stress–life, strain–life, or FS–life), as specified. LDR for the two-level step tests is represented by:

$$\frac{n_1}{N_{f_1}} + \frac{n_2}{N_{f_2}} = 1 \tag{2}$$

Significant hardening was observed at the lower level as shown in Fig. 8. This figure represents the stress response in strain control (Fig. 8a) and strain response in load control (Fig. 8b) for high–low step tests. For comparison purposes, constant amplitude fully reversed responses are also presented. The amount of hardening increased with increasing the number of cycles applied at the higher level. In load control, hardening led to a reduction in strain amplitude of the second level.

With regards to fatigue life, load sequence effect was observed. Cycle ratios calculated with the LDR based on strain–life curve for strain-controlled tests and stress–life curve for load-controlled tests can be seen in Fig. 9 and Table 3. As can be seen, shorter lives were obtained in strain-controlled tests, as compared to load-controlled tests.

Microcracks initiated during the first higher level and grow during the lower second step. Microcracks mentioned here are small cracks and do not affect the overall mechanical behavior of the material. Most cracks were perpendicular to the loading direction, and were about one hundred to several hundred micrometers long. Numerous cracks were observed.

Although similar trends in hardening behavior were observed in strain control and load control, the control mode had a strong influence on the outcome of the step tests (similar to pre-strain tests previously discussed). In strain control, hardening induced by the first strain level led to smaller cycle ratios (i.e., shorter lives) due to higher stress amplitudes at the second strain level. In

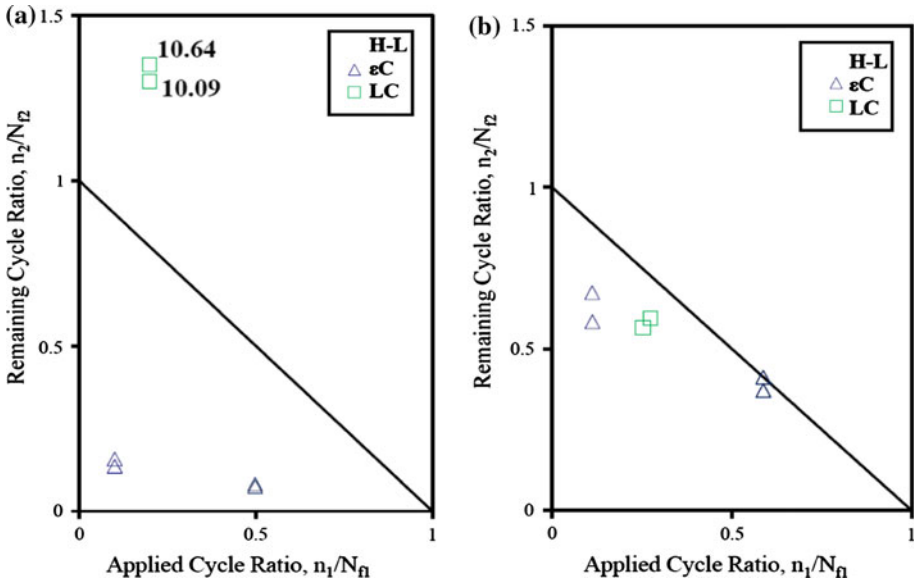

Fig. 9 Cycle ratios in high–low (H–L) step tests using (**a**) strain–life or stress–life curve and (**b**) FS curve. The line in each figure represents linear damage rule (LDR)

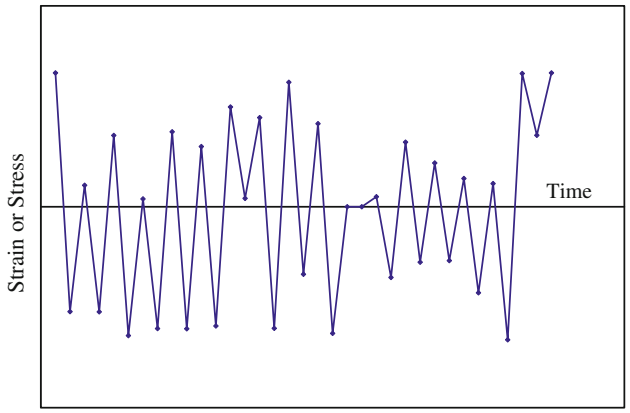

Fig. 10 Loading history used for random loading tests

load-controlled tests, however, the hardening induced by the first load level resulted in smaller strain amplitude at the second load level, leading to larger cycle ratios, as shown in Fig. 9a. Cycle ratios referred to here were calculated using the common approach of utilizing LDR with a strain–life curve in strain control, or with a stress–life curve in load control. This type of damage accumulation calculation can lead to erroneous conclusions, however, as high–low (H–L) sequence fatigue life is over-predicted in strain control and under-predicted in load control. To circumvent this shortcoming, parameters including both stress and strain, such as FS or SWT parameters can be used for damage accumulation calculations. The LDR was used with the FS parameter with results presented in Fig. 9b. Significant improvement is observed using the FS parameter. As seen in Table 3 and Fig. 9b, damage ratios for these tests are closer to unity using the FS parameter. Neither the strain–life nor the stress–life approach account for the hardening due to the higher load level in H–L step tests.

Random loading tests

For RL tests, the loading history used is shown in Fig. 10, which was Rainflow cycle counted. The history was amplified to reach the desired maximum and minimum strain or stress values in the block as presented in Table 4. RL tests were conducted on virgin, as well as on pre-strained specimens, and in both strain control and load control.

For pre-strained tests, higher stress amplitudes (by about 10%) were observed in strain control and fatigue lives were shorter (by more than a factor of 4) than the virgin material test at the same strain level. However, in load control, pre-hardening led to a reduction in strain amplitude (by 50%) compared to the virgin specimen test and a significant increase in fatigue life (by more than a factor of 7).

Damage accumulation was computed using LDR combined with strain–life, stress–life, and FS curves. Life predictions are presented in Table 4 and also in Fig. 11, where predicted versus experimental lives are plotted. Scatter bands of ± 2 and ± 5 are also shown in Fig. 11. As can be seen, the FS parameter improves the predictions as compared to the more common strain–life or stress–life approach. This is due to strong deformation history effect in stainless steel 304L, where including both stress and strain in damage calculations leads to more accurate results.

Conclusions

(1) Significant cyclic hardening is observed for stainless steel 304L, leading to cyclic deformation response of this material to be strongly affected by prior higher

Table 4 Summary of random loading tests results

Test control mode	ε_{max} (%)	ε_{min} (%)	σ_{max} (MPa)	σ_{min} (MPa)	Experimental number of blocks to failure	Predicted number of blocks to failure (ε–N or S–N)	Predicted number of blocks to failure (FS–N)
Virgin specimens							
Strain	0.995	−1.00	410	−403	230	233	198
Strain	1.00	−1.00	406	−398	243	235	202
Strain	0.497	−0.494	315	−313	2,998	4,181	3,101
Strain	0.498	−0.496	302	−296	2,688	4,110	3,248
Strain	0.290	−0.289	273	−273	>103,242	145,254	77,100
Load	0.635	−0.194	284	−278	13,870	8,348	14,258
Load	0.409	−0.393	278	−273	14,892	10,264	17,707
Pre-strained[a] specimens							
Strain	0.287	−0.286	307	−297	26,550	155,233	61,864
Strain	0.288	−0.287	308	−296	21,144	152,711	61,279
Load	−0.084	−0.487	281	−279	>100,000	8,126	767,000

[a] For pre-strained tests, 10 cycles at 2% strain amplitude were applied

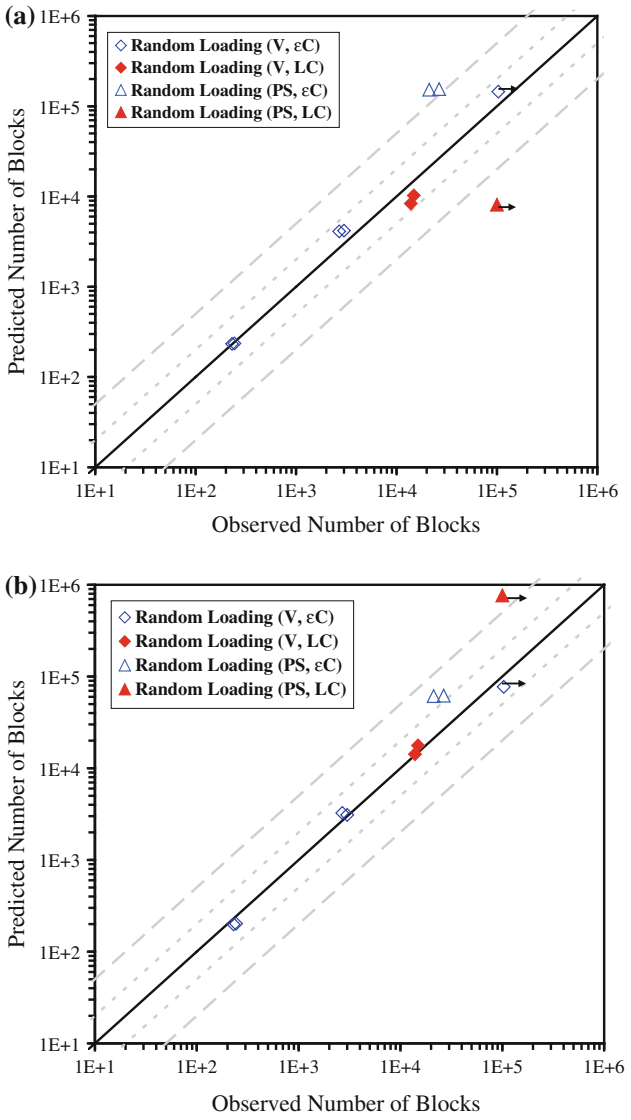

Fig. 11 Predicted versus experimental lives using LDR (**a**) strain–life or stress–life curve and (**b**) FS curve

amplitude cycles (i.e., strong deformation history effect).

(2) Load-controlled test fatigue lives were similar to strain-controlled test fatigue lives, showing no effect of the load control mode on fully reversed fatigue behavior.

(3) In strain-controlled mean strain tests, due to the considerable amount of plasticity the mean stress relaxed to very small values during the first few percent of the fatigue life. In spite of mean stress relaxation and contrary to expectations, fatigue lives of tensile mean strain tests were much shorter and fatigue lives of compressive mean strain tests were much longer than those in fully reversed tests.

(4) The effect of PS on fatigue life was dependent on the test control mode. PS led to significantly shorter life in strain-controlled tests, but significantly longer life in load-controlled test, as compared with the virgin material. These observations were made in both constant amplitude as well as in RL tests.

(5) Strong ferro-magnetic properties, typically associated with martensitic transformation and believed to result from accumulation of plastic strain, were observed for specimens with or without secondary hardening. Micro-hardness measurements revealed strong heterogeneity of the gage section, attributed to such transformation. However, secondary hardening may be due to the formation of an alternate structure, rather than or in addition to the martensitic transformation. PS can induce sufficient initial hardening to prevent or hinder additional alterations of the microstructure.

(6) In H–L step tests, significant hardening was observed at the lower step level. The level of hardening increased with increasing the number of cycles applied at the higher level. Due to significant hardening resulting from the high level, test control mode had a strong influence on fatigue life. Load-controlled tests presented much longer lives than strain-controlled tests.

(7) Due to significant hardening and strong deformation history effects, a fatigue life parameter with both stress and strain terms is necessary to correlate the stainless steel data with deformation history effects. While the conventional strain–life or stress–life curves can result in inaccurate life predictions, the FS parameter as such a parameter was shown to lead to significantly better fatigue life correlations.

References

1. Lieurade HP, Ribes A, Bollinger E (1986) Mém Etudes Sci Rev Métall 83:547
2. Baudry G, Pineau A (1977) Mater Sci Eng 28:229
3. Gerland M, Alain R, Ait Saadi B, Mendez J (1997) Mater Sci Eng A229:68
4. Khan Z, Ahmed M (1996) J Mater Eng Perform 5:201
5. Lehéricy Y, Mendez J (2006) In: 9th International fatigue congress, Atlanta, GA
6. Stephens RI, Fatemi A, Stephens RR, Fuchs HO (2000) Metal fatigue in engineering. Wiley Inter-Science, New York
7. Fatemi A, Yang L (1998) Int J Fatigue 20:9
8. Colin J, Fatemi A, Taheri S (2010) J Eng Mater Technol Trans ASME 132(2):021008
9. Colin J, Fatemi A (2010) J Fatigue Fract Eng Mater Struct 33(4):205
10. Smith KN, Watson P, Topper TH (1970) J Mater 5:767
11. Fatemi A, Socie DF (1988) Fatigue Fract Eng Mater Struct 11:149
12. Lebedev AA, Kosarchuk VV (2000) Int J Plast 16:749

13. Kaleta J, Zietek G (1998) Fatigue Fract Eng Mater Struct 21:955
14. Krauss G (2005) Steels: processing, structure, and performance, 3rd edn. ASM International, Materials Park, p 508
15. Nagy E, Mertinger V, Tranta F, Solyom J (2004) Mater Sci Eng A 378:308
16. Qian J, Fatemi A (1995) Int J Fatigue 17:15